

## Article

# Utilization of Metallurgy—Beneficiation Combination Strategy to Decrease TiO<sub>2</sub> in Titanomagnetite Concentrate before Smelting

Pan Chen <sup>1,2</sup>, Yameng Sun <sup>1,2</sup>, Lei Yang <sup>1,2</sup>, Rui Xu <sup>1,2</sup>, Yangyong Luo <sup>3</sup>, Xianyun Wang <sup>3</sup>, Jian Cao <sup>1,2,4,\*</sup>   
and Jinggang Wang <sup>1,2,\*</sup>

<sup>1</sup> School of Minerals Processing and Bioengineering, Central South University, Changsha 410083, China; panchen@csu.edu.cn (P.C.); sunyameng11@126.com (Y.S.); lei\_yang@csu.edu.cn (L.Y.); 18370956193@163.com (R.X.)

<sup>2</sup> Key Laboratory of Hunan Province for Clean and Efficient Utilization of Strategic Calcium-Containing Mineral Resources, Central South University, Changsha 410083, China

<sup>3</sup> Sichuan Anning Iron and Titanium Co., Ltd., Panzhihua 617200, China; chychjack@foxmail.com (Y.L.); wangxianyun@163.com (X.W.)

<sup>4</sup> State Key Laboratory of Mineral Processing, Beijing 100814, China

\* Correspondence: caojianlzu@163.com (J.C.); cu18535601121@163.com (J.W.);  
Tel./Fax: +86-731-88830482 (J.C. & J.W.)

**Abstract:** Excessive TiO<sub>2</sub> in titanomagnetite concentrates (TC) causes unavoidable problems in subsequent smelting. At present, this issue cannot be addressed using traditional mineral processing technology. Herein, a strategy of metallurgy-beneficiation combination to decrease the TiO<sub>2</sub> grade in TC before smelting was proposed. Roasting TC with calcium carbonate (CaCO<sub>3</sub>) together with magnetic separation proved to be a viable strategy. Under optimal conditions (roasting temperature = 1400 °C, CaCO<sub>3</sub> ratio = 20%, and magnetic intensity = 0.18 T), iron and titanium was separated efficiently (Fe grade: 56.6 wt.%; Fe recovery: 70 wt.%; TiO<sub>2</sub> grade 3 wt.%; TiO<sub>2</sub> removal: 84.1 wt.%). X-ray diffraction, scanning electron microscopy, and energy dispersive spectroscopy analysis were used to study the mechanisms. The results showed that Ti in TC could react with CaO to form CaTiO<sub>3</sub>, and thermodynamic calculations provided a relevant theoretical basis. In sum, the metallurgy-beneficiation combination strategy was proven as an effective method to decrease unwanted TiO<sub>2</sub> in TC.

**Keywords:** titanomagnetite concentrate; metallurgy-beneficiation combination; roasting; magnetic separation



**Citation:** Chen, P.; Sun, Y.; Yang, L.; Xu, R.; Luo, Y.; Wang, X.; Cao, J.; Wang, J. Utilization of Metallurgy—Beneficiation Combination Strategy to Decrease TiO<sub>2</sub> in Titanomagnetite Concentrate before Smelting. *Minerals* **2021**, *11*, 1419. <https://doi.org/10.3390/min11121419>

Academic Editor: Frédéric J. Doucet

Received: 10 November 2021

Accepted: 10 December 2021

Published: 15 December 2021

**Publisher's Note:** MDPI stays neutral with regard to jurisdictional claims in published maps and institutional affiliations.



**Copyright:** © 2021 by the authors. Licensee MDPI, Basel, Switzerland. This article is an open access article distributed under the terms and conditions of the Creative Commons Attribution (CC BY) license (<https://creativecommons.org/licenses/by/4.0/>).

## 1. Introduction

As high-grade iron ores are gradually depleted, titanomagnetite is used as an alternative ore for steel smelting [1,2]. However, due to a unique crystal structure, the TiO<sub>2</sub> grade in titanomagnetite concentrate (TC) is inevitably increased, which results in problems such as liquidus temperature increase, decrease in the reduction effect of the ore, and viscous smelting slag [3–8]. In the traditional steel industry, additional ordinary iron ore is mixed with the TC at a high proportion to decrease the TiO<sub>2</sub> grade, but it cannot prevent undesired TiO<sub>2</sub> in TC [9].

The improvement in the smelting process of TC with high-grade TiO<sub>2</sub> has become an important research topic. For example, direct reduction-electric furnace smelting is used in South Africa and New Zealand. However, for this method, the grade of titanium in TC must be under 1% [10]. Direct reduction-magnetic separation smelting is also well-developed, but its disadvantage is that it requires high temperatures to meet the high metallization degree [11]. Additionally, sodium salt-roasting direct reduction is used in smelting, but this process consumes a large amount of sodium salt, resulting in high cost [12,13]. The high reaction temperature (1250–1350 °C) of reduction roasting also causes a series of side

reactions, such as the formation of solid solutions (brookite ( $\text{Fe}_2\text{TiO}_5$ ) and black titanium ( $\text{FeTi}_2\text{O}_5$ )) [14,15]. Moreover, titanium oxide will be reduced to TiC, TiN, and other high-melting but low-value substances in a reducing atmosphere, resulting in an increase in the viscosity of the new phase [16–18]. The problem in the smelting of TC with high-grade  $\text{TiO}_2$  has not been solved completely, and as a result, a new strategy that can reduce  $\text{TiO}_2$  grade in TC before smelting must be developed.

In this work, a metallurgy-beneficiation combination strategy to decrease  $\text{TiO}_2$  was proposed. TC (Panzhihua, magmatic titanomagnetite) was roasted with calcium carbonate ( $\text{CaCO}_3$ ) under oxidizing atmosphere, and the roasted product after phase transformation was subjected to magnetic separation.  $\text{CaCO}_3$  is one of the most common substances on earth. It is found in rocks such as marble and calcite. It is cheap and distributes widely. X-ray diffraction (XRD), scanning electron microscopy (SEM), and energy dispersive spectroscopy (EDS) analysis were used to study the mechanisms, and thermodynamic calculations provided a clear theoretical basis.

## 2. Materials and Methods

### 2.1. Materials and Reagents

The experimental TC powder in this investigation was obtained from Panzhihua (Sichuan Province, China). The TC sample was characterized using chemical analysis (titration), and the results are shown in Table 1. The Fe and  $\text{TiO}_2$  grades were 54.4 wt.% and 13.1 wt.%, respectively.

**Table 1.** Chemical analysis of TC sample (wt.%).

Element	Fe	$\text{TiO}_2$	MgO	$\text{Al}_2\text{O}_3$	$\text{SiO}_2$	CaO
Content	54.5	13.1	2.5	3.4	3.2	1

The sample (85 wt.% passing  $0.074\ \mu\text{m}$ ) was air-dried. Analytically pure  $\text{CaCO}_3$  was supplied by Sinopharm Chemical Reagent, Changsha, China. Tap water was used in the magnetic separation tests.

### 2.2. Roasting and Magnetic Separation Tests

A Vacuum Atmosphere Box Furnace (GF17Q-III, Tianjin Mafur Technology Co. Ltd., Tianjin, China.) was used for the roasting process. Before roasting, 100 g of TC powder was mixed with specific proportions of  $\text{CaCO}_3$ , placed into the corundum crucible, and roasted at specific temperatures for 5 h to complete the reaction. After roasting, the samples were cooled to room temperature by water quenching.

After the roasted materials were ground (95 wt.% passing  $38\ \mu\text{m}$ ) in a ball mill (XMQ- $\Phi 150 \times 50$ , Nanchang Haifeng Mining Machinery Equipment Co., Ltd., Nanchang, China.), the magnetic separation experiments with different magnetic intensities were performed on a magnetic separator tube (XCGS74- $\phi 50$ , Jiangxi Shicheng Yongsheng Mineral Processing Equipment Manufacturing Co. Ltd., Shicheng, China.) (flow: 1.2 L/min; stroke: 70 times/min). The magnetic product (iron concentrate) and nonmagnetic product (tailing) were filtered, dried, weighed, and analyzed for Fe and  $\text{TiO}_2$ , and the mass balances were made to obtain the Fe and  $\text{TiO}_2$  recovery values [19]. Three sets of parallel experiments were set up for each condition experiment. Error bars in the experimental results represent one standard deviation of uncertainty obtained from three independent runs.

### 2.3. XRD Analysis

The solid-phase structure was analyzed by XRD (X' Pert PRO MPD, Nalytical Co. Ltd., Amsterdam, The Netherlands) with  $\text{Cu K}\alpha$  radiation. The operating voltage and current were 40 kV and 40 mA, respectively. The diffraction angle was scanned from  $10^\circ$  to  $70^\circ$ , and the scanning speed was  $8^\circ/\text{min}$ .

## 2.4. SEM-EDS Measurement

An SU1510 scanning electron microscope (Hitachi Company, Tokyo, Japan) equipped with an energy-dispersive X-ray spectrometer was used to analyze the prepared samples under an accelerating voltage of 20 kV. The analyzed TC samples are raw ore and roasted ore, obtained under optimal conditions ( $\text{CaCO}_3$  ratio = 20%, roasting temperature = 1400 °C, without magnetic separation).

## 3. Results

### 3.1. Roasting and Magnetic Separation Tests

In the roasting and magnetic separation processes, the main factors affecting  $\text{TiO}_2$  grade were roasting temperature,  $\text{CaCO}_3$  ratio, and magnetic intensity [20]. Temperature determines the phase transition of the roasting sample. As shown in Figure 1a,b, an increased roasting temperature would increase Fe recovery. At 1400 °C, the Fe grade was the highest (56.6 wt.%), whereas the  $\text{TiO}_2$  grade in the roasted materials was the lowest (4.5 wt.%), and compared with TC, the removal exceeded 80%. Then, the three indicators decreased to varying degrees, which were attributed to the phase transformation of magnetic iron to nonmagnetic iron in the oxidizing atmosphere [20]. Therefore, 1400 °C was the chosen firing temperature for subsequent experiments.

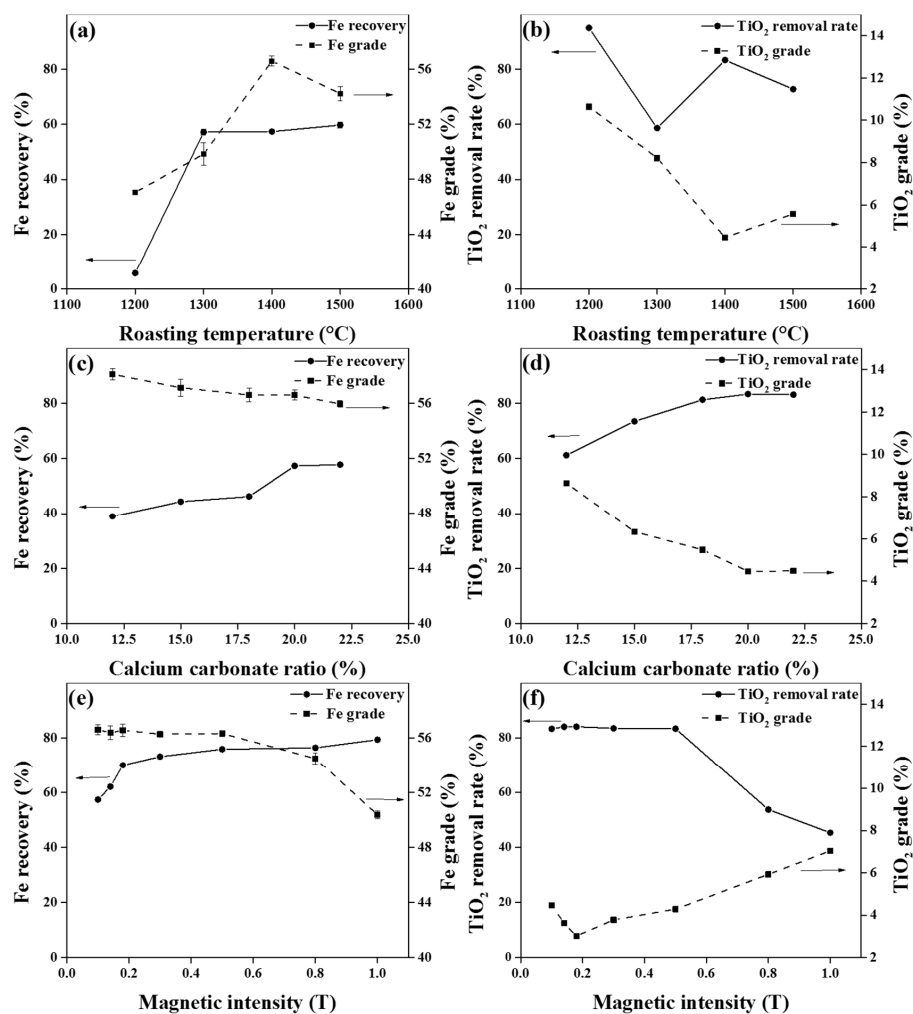


**Figure 1.** The recovery and grade of Fe and the removal and grade of  $\text{TiO}_2$  under different roasting temperatures (a,b),  $\text{CaCO}_3$  ratio (c,d) and magnetic intensity (e,f). (Above experiments were performed via changing corresponding condition and fixing other two conditions. The fixed conditions selected from the following values: roasting temperature = 1400 °C,  $\text{CaCO}_3$  ratio = 20%, Magnetic intensity = 0.1 T).

A proper  $\text{CaCO}_3$  ratio could save cost and ensure the expected result. As shown in Figure 1c,d, the increase in  $\text{CaCO}_3$  ratio reduced the  $\text{TiO}_2$  grade in the magnetic concentrate and increased Fe recovery and the removal of  $\text{TiO}_2$ , which was in line with the expected goal. However, the Fe grade slightly decreased, which might be attributed to the insufficient separation of CaO from the magnetic iron [21]. Under the  $\text{CaCO}_3$  ratio of 20%, the separation efficiency of iron and titanium was the best (Fe grade: 56.6 wt.%; Fe recovery: 57.4 wt.%;  $\text{TiO}_2$  grade 4.5 wt.%;  $\text{TiO}_2$  removal: 83.4 wt.%). Hence, the  $\text{CaCO}_3$  ratio of 20% was selected as the optimal condition for the following tests.

Magnetic intensity was the decisive factor in obtaining the final magnetic concentrate. Figure 1e,f shows that with the increase in magnetic intensity, the grade of Fe and the removal of  $\text{TiO}_2$  decreased, while the recovery of Fe slowly increased, and an inflection point of the grade of  $\text{TiO}_2$  was present. These results were attributed to the following reasons: (1) Effective recovery of magnetic concentrate requires a magnetic field with an optimal intensity [22–24]. (2) Excessive magnetic intensity caused unwilling entrainment for separation [25–27]. Meanwhile, 0.18 T was the optimal magnetic intensity for efficient separation. The grade and recovery of Fe were 56.6 wt.% and 70 wt.%, respectively, and the grade and removal of  $\text{TiO}_2$  were 3 wt.% and 84.1 wt.%, respectively. Such roasted product was beneficial to the smelting process, although the recovery of Fe was lower than that obtained under other experimental conditions [28,29].

### 3.2. Investigation of Fe-Ti Separation Mechanism

XRD and SEM-EDS analysis were used to explore the separation mechanism of Fe-Ti during sintering.

#### 3.2.1. XRD Analysis

XRD spectra and chemical composition of roasted sample obtained under optimum control conditions (roasting temperature = 1400 °C,  $\text{CaCO}_3$  ratio = 20%, magnetic intensity = 0.18 T) are shown in Figure 2 and Table 2, respectively. Almost all ilmenite ( $\text{FeTiO}_3$ ) in the TC was converted to perovskite ( $\text{CaTiO}_3$ ) after roasting with  $\text{CaCO}_3$  at 1400 °C (Figure 2c), which was consistent with previous findings [30,31]. The main compositions of nonmagnetic tailing (Figure 2a) were hematite, perovskite, and pyroxene, and the main compositions of magnetic concentrate (Figure 2b) were magnetite and hematite. These results indicated that TC could be roasted with  $\text{CaCO}_3$  to obtain a nonmagnetic perovskite, which could be processed by magnetic separation. Finally, Fe grade increased from 54.4 wt.% to 56.6 wt.%, and  $\text{TiO}_2$  grade decreased dramatically from 13.1 wt.% to 3 wt.% in the magnetic concentrate.

**Table 2.** Chemical analysis of experimental samples (wt.%).

Element	Fe	Recovery	$\text{TiO}_2$	Recovery	$\text{SiO}_2$	Recovery	CaO	Recovery
TC	54.4	-	13	-	3.1	-	1	-
Roasted	49	-	11.5	-	2.9	-	10.5	-
Concentrate	56.6	70	3	15.9	1.5	19.9	6.8	17.5
Tailing	37.4	30	24.6	84.1	5.2	80.2	16.4	82.5

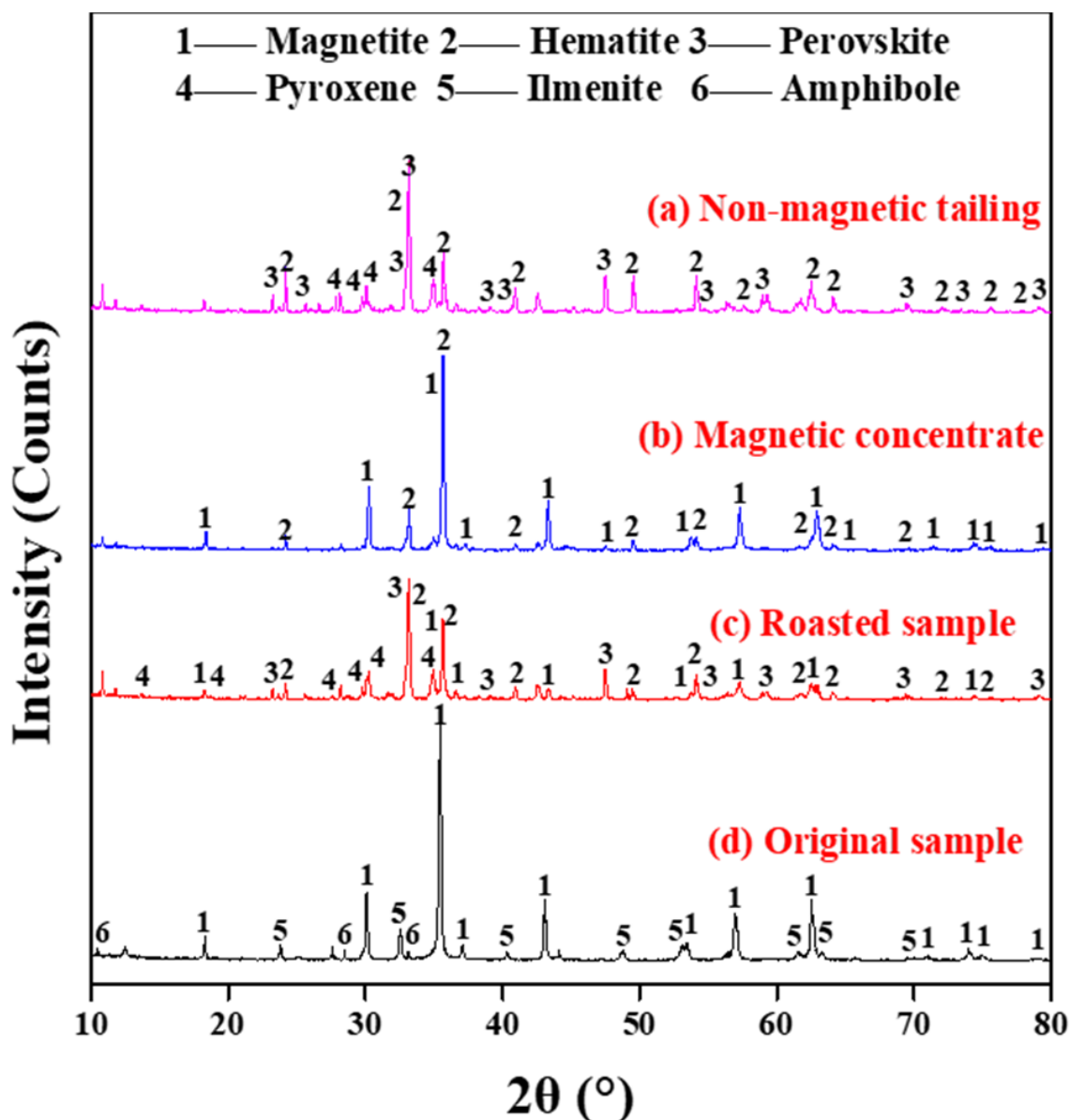
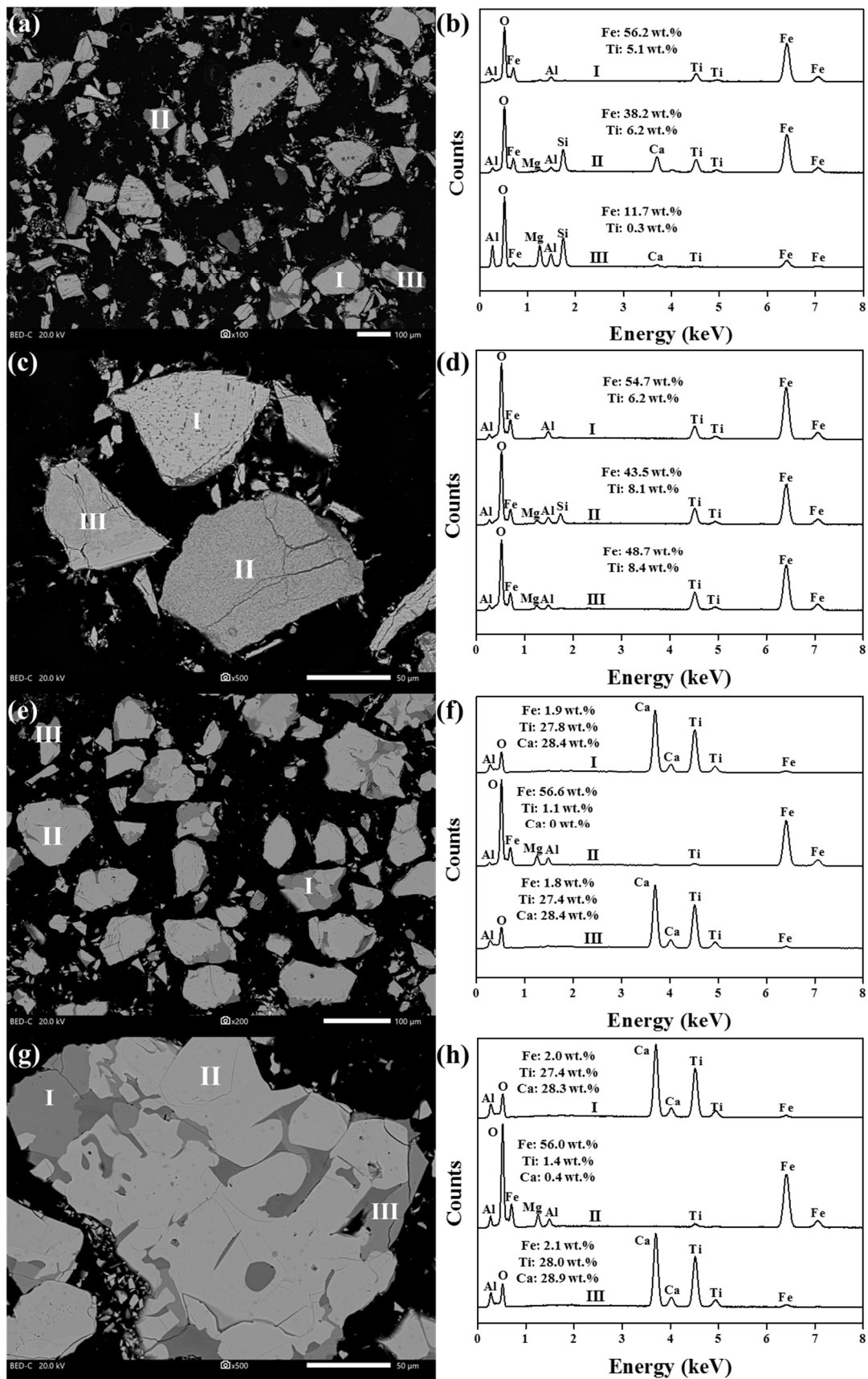


Figure 2. XRD spectrum of the non-magnetic tailing (a), magnetic concentrate (b), roasted sample (c) and original sample (d).

### 3.2.2. SEM-EDS Analysis

Ti and Fe coexist in a similar phase in the crystal lattice of TC, which is the reason for the difficult Fe-Ti separation [32–34]. SEM-EDS analysis of TC under different multiples was performed for visual observation (Figure 3 ((a,b)  $\times 100$ , (c,d)  $\times 500$ )). The elements in the bright area were mainly Fe, Ti, and O, which were attributed to the  $\text{FeTiO}_3$  in TC, while the species in the dark area were mainly miscellaneous elements (Mg, Al, Si, and O). For mineral particles less than  $30\ \mu\text{m}$ , the obvious monomer dissociation of  $\text{TiO}_2$  and  $\text{Fe}_3\text{O}_4$  was difficult to observe, which was consistent with previous studies [35]. As such, the efficient separation of complicated Fe-Ti association in the TC was extremely difficult.



**Figure 3.** SEM-EDS analysis of TC (a–d) and roasted sample (e–h) under different multiples ((a,b) × 100, (e,f) × 200, (c,d) and (g,h) × 500, the roman numerals in the SEM images denote the testing area used for EDS).

The SEM-EDS images of roasted samples under different multiples are shown in Figure 3 ((e,f)  $\times 200$ , (g,h)  $\times 500$ ). The main elements in the bright area (II) were Fe and O, and the grade of Ti was less than 2 wt.%. In the gray areas (I and III), the grade of Ti and Ca were both approximately 28 wt.%, which was attributed to  $\text{CaTiO}_3$  formation [36] and consistent with the results of XRD analysis. Meanwhile, the size of the iron-phase species also directly affected the subsequent magnetic separation of Fe-Ti [36]. Figure 3e shows that the size of the iron phase particles generally exceeded 50  $\mu\text{m}$ , and the size of the Ti phase particles ( $\text{CaTiO}_3$ ) was distributed in the range 10–50  $\mu\text{m}$ , which met the magnetic separation requirements.

### 3.3. Thermodynamic Analysis

The reaction equation module in the thermodynamic software HSC Chemistry 6.0 was used to calculate the standard Gibbs free-energy change in the experimental reaction, to reveal the reactions that occurred during the roasting process [37]. Possible reactions are known by reviewing the literature [38]. The primary reactions during roasting of TC are summarized as follows:

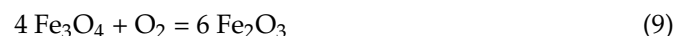
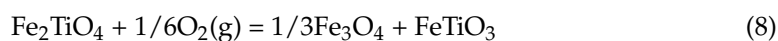
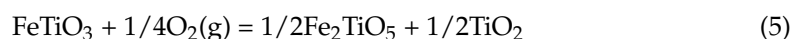
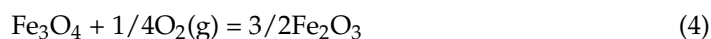
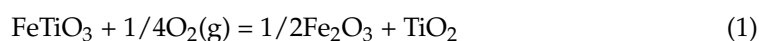
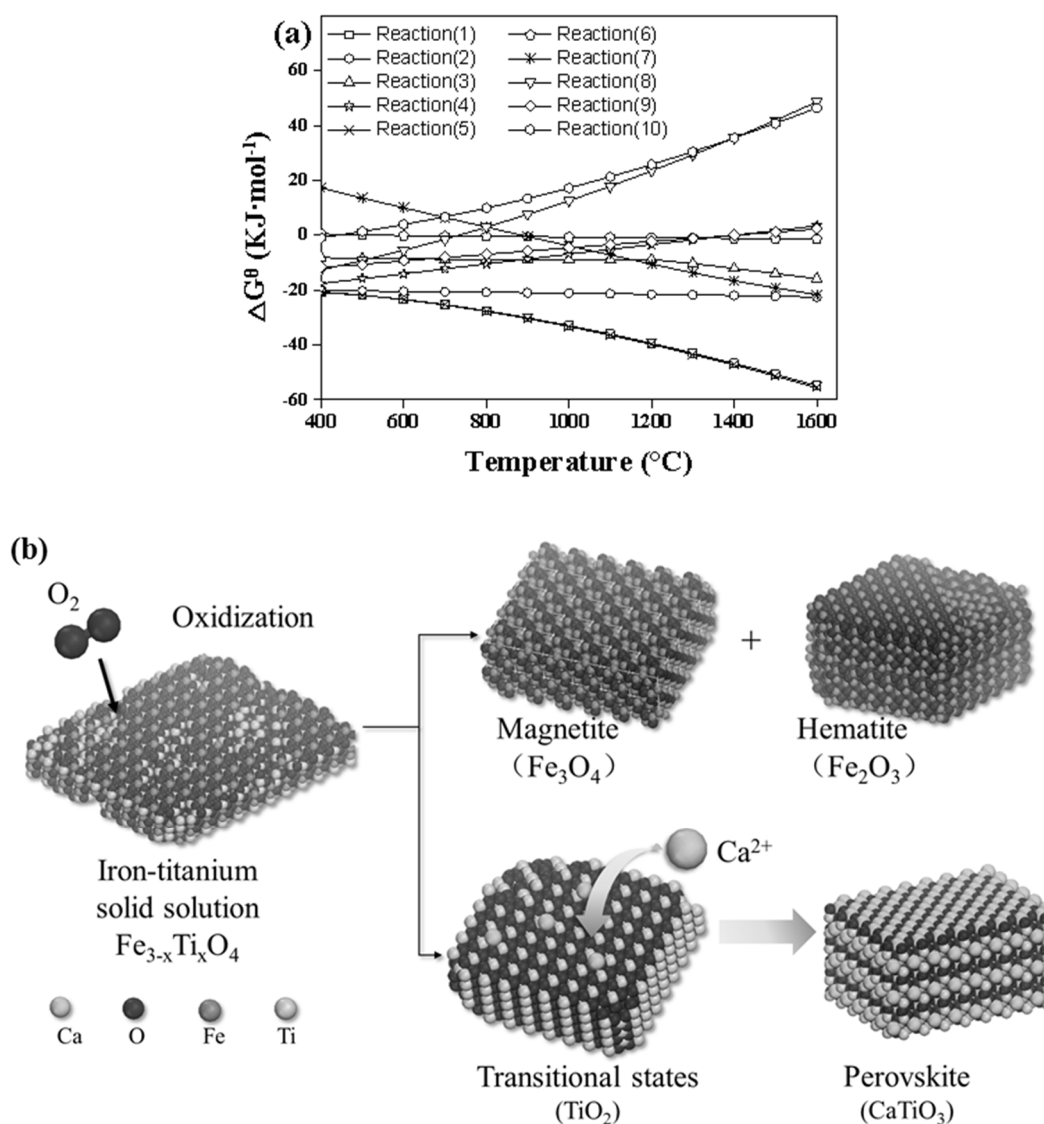


Figure 4a shows the relationships between the change in Gibbs free energy and the temperature of reactions (1)–(10). The thermodynamic feasibility of  $\text{FeTiO}_3$  reacting with  $\text{O}_2$  to generate  $\text{Fe}_2\text{O}_3$  or  $\text{Fe}_2\text{TiO}_5$  was almost the same, and the two reactions generated  $\text{TiO}_2$ . Meanwhile, under the same condition, the Gibbs free energy of reaction between  $\text{TiO}_2$  and  $\text{CaO}$  was far lower than that of the reaction between  $\text{TiO}_2$  and  $\text{Fe}_2\text{O}_3$ . Thus,  $\text{TiO}_2$  preferred to react with  $\text{CaO}$  to generate perovskite, which was consistent with the experimental results. Thermodynamic calculations theoretically support the feasibility of this strategy.

The ore-phase transformation of iron-titanium solid solution via oxidation is shown in Figure 4b. Adding  $\text{CaCO}_3$  into the roasting system under the oxidizing atmosphere resulted in the phase-changed reaction of the iron-titanium solid solution ore in the TC to produce  $\text{CaTiO}_3$ ,  $\text{Fe}_2\text{O}_3$ ,  $\text{Fe}_3\text{O}_4$ , and other iron- and titanium-independent minerals [39]; thus, iron and titanium were released in the solid solution lattice. Meanwhile, the perovskite phase was stable, and the lattice structure had a low degree of close packing, strong brittleness, and weak adhesion strength to the iron phase [40], thereby resulting in favorable conditions for the further magnetic separation of iron and titanium.



**Figure 4.** (a) Relationships between the change of Gibbs free energy and the temperature of reactions (1)–(10). (b) Ore phase transformation of iron-titanium solid solution oxidation.

#### 4. Conclusions

In this work, a metallurgy-beneficiation combination strategy to decrease  $\text{TiO}_2$  in TC was proposed. The effects of roasting temperature,  $\text{CaCO}_3$  ratio, and magnetic intensity on the separation efficiency of iron and titanium were studied to achieve the efficient separation of iron and titanium in TC via oxidative phase change. Experimental results showed that under optimal conditions (roasting temperature = 1400 °C,  $\text{CaCO}_3$  ratio = 20%, and magnetic intensity = 0.18 T), iron and titanium could be separated efficiently (Fe grade: 56.6 wt.%; Fe recovery: 70 wt.%;  $\text{TiO}_2$  grade 3 wt.%;  $\text{TiO}_2$  removal: 84.1 wt.%). XRD, SEM-EDS, and thermodynamic calculations showed that in an oxidizing atmosphere, TC could be oxidized to  $\text{TiO}_2$ , and CaO preferentially reacted with  $\text{TiO}_2$  to form perovskite ( $\text{CaTiO}_3$ ) due to the small Gibbs free energy.

**Author Contributions:** Conceptualization, Y.L. and X.W.; methodology, R.X.; software, L.Y.; validation, J.W., Y.S. and P.C.; formal analysis, J.C.; investigation, Y.S.; resources, J.W.; data curation, J.C.; writing—original draft preparation, P.C. and Y.S.; writing—review and editing, P.C. and Y.S.; visualization, J.W.; supervision, J.C.; project administration, J.C. and J.W.; funding acquisition, J.C. and J.W. All authors have read and agreed to the published version of the manuscript.

**Funding:** This research was funded by National Key R&D Program of China (2019YFC1803500), Natural Science Foundation of China (52074357, 52004336), Hunan Provincial Natural Science Foundation (2020JJ5714, 2018JJ3665), China Postdoctoral Science Foundation (2019M650188). Funded by Open Foundation of State Key Laboratory of Mineral Processing (BGRIMM-KJSKL-2021-06), Graduate Research Innovation Project of Central South University (2021zzts0888), the Project of Vanadium titanium Industry Alliance.

**Acknowledgments:** The authors acknowledge the support of National Key R&D Program of China (2019YFC1803500), Natural Science Foundation of China (52074357, 52004336), Hunan Provincial Natural Science Foundation (2020JJ5714, 2018JJ3665), China Postdoctoral Science Foundation (2019M650188). Funded by Open Foundation of State Key Laboratory of Mineral Processing (BGRIMM-KJSKL-2021-06). Graduate Research Innovation Project of Central South University (2021zzts0888), the Project of Vanadium titanium Industry Alliance.

**Conflicts of Interest:** The authors declare no conflict of interest.

## References

1. Li, H.M.; Li, L.X.; Yang, X.Q.; Cheng, Y.B. Types and geological characteristics of iron deposits in China. *J. Asian Earth Sci.* **2015**, *103*, 2–22. [[CrossRef](#)]
2. Gao, F.; Olayiwola, A.U.; Liu, B.; Wang, S.; Du, H.; Li, J.; Wang, X.; Chen, D.; Zhang, Y. Review of Vanadium Production Part I: Primary Resources. *Miner. Process. Extr. Metall. Rev.* **2021**, *15*, 1–23. [[CrossRef](#)]
3. Lv, X.; Lun, Z.; Yin, J.; Bai, C. Carbothermic reduction of vanadium titanomagnetite by microwave irradiation and smelting behavior. *ISIJ Int.* **2013**, *53*, 1115–1119. [[CrossRef](#)]
4. He, S.; Sun, H.; Tan, D.; Peng, T. Recovery of Titanium Compounds from Ti-enriched Product of Alkali Melting Ti-bearing Blast Furnace Slag by Dilute Sulfuric Acid Leaching. *Procedia Environ. Sci.* **2016**, *31*, 977–984. [[CrossRef](#)]
5. Fu, W.-g.; Wen, Y.-c.; Xie, H.-e. Development of Intensified Technologies of Vanadium-Bearing Titanomagnetite Smelting. *J. Iron Steel Res. Int.* **2011**, *18*, 7–10. [[CrossRef](#)]
6. Gao, Y.; Bian, L.; Liang, Z. Influence of B<sub>2</sub>O<sub>3</sub> and TiO<sub>2</sub> on viscosity of titanium-bearing blast furnace slag. *Steel Res. Int.* **2015**, *86*, 386–390. [[CrossRef](#)]
7. Li, W.; Wang, N.; Fu, G.; Chu, M.; Zhu, M. Influence of TiO<sub>2</sub> addition on the oxidation induration and reduction behavior of Hongge vanadium titanomagnetite pellets with simulated shaft furnace gases. *Powder Technol.* **2018**, *326*, 137–145. [[CrossRef](#)]
8. Li, W.; Fu, G.Q.; Chu, M.S.; Zhu, M.Y. Gas-Based Direct Reduction of Hongge Vanadium Titanomagnetite-Oxidized Pellet and Melting Separation of the Reduced Pellet. *Steel Res. Int.* **2017**, *88*, 1–10. [[CrossRef](#)]
9. Sachkov, V.I.; Nefedov, R.A.; Orlov, V.V.; Medvedev, R.O.; Sachkova, A.S. Hydrometallurgical processing technology of titanomagnetite ores. *Minerals* **2018**, *8*, 2. [[CrossRef](#)]
10. Wang, S.; Guo, Y.-f.; Jiang, T.; Chen, F.; Zheng, F.-q.; Tang, M.-j.; Yang, L.-z.; Qiu, G.-z. Appropriate titanium slag composition during smelting of vanadium titanomagnetite metallized pellets. *Trans. Nonferrous Met. Soc. China* **2018**, *28*, 2528–2537. [[CrossRef](#)]
11. Zhao, L.S.; Wang, L.N.; Chen, D.S.; Zhao, H.X.; Liu, Y.H.; Qi, T. Behaviors of vanadium and chromium in coal-based direct reduction of high-chromium vanadium-bearing titanomagnetite concentrates followed by magnetic separation. *Trans. Nonferrous Met. Soc. China* **2015**, *25*, 1325–1333. [[CrossRef](#)]
12. Samanta, S.; Mukherjee, S.; Dey, R. Upgrading Metals Via Direct Reduction from Poly-metallic Titaniferous Magnetite Ore. *JOM* **2015**, *67*, 467–476. [[CrossRef](#)]
13. Liu, X.J.; Chen, D.S.; Chu, J.L.; Wang, W.J.; Li, Y.L.; Qi, T. Recovery of titanium and vanadium from titanium–vanadium slag obtained by direct reduction of titanomagnetite concentrates. *Rare Met.* **2015**, *6*, 1–9. [[CrossRef](#)]
14. Wan, J.; Du, H.; Gao, F.; Wang, S.; Gao, M.; Liu, B.; Zhang, Y. Direct Leaching of Vanadium from Vanadium-bearing Steel Slag Using NaOH Solutions: A Case Study. *Miner. Process. Extr. Metall. Rev.* **2021**, *42*, 257–267. [[CrossRef](#)]
15. Wen, J.; Jiang, T.; Liu, Y.; Xue, X. Extraction Behavior of Vanadium and Chromium by Calcification Roasting-Acid Leaching from High Chromium Vanadium Slag: Optimization Using Response Surface Methodology. *Miner. Process. Extr. Metall. Rev.* **2019**, *40*, 56–66. [[CrossRef](#)]
16. Wang, J.; Wang, W.; Ai, Z.; Li, M.; Li, H.; Peng, W.; Zhao, Y.; Song, S. Adsorption toward Pb(II) occurring on three-dimensional reticular-structured montmorillonite hydrogel surface. *Appl. Clay Sci.* **2021**, *210*, 106153. [[CrossRef](#)]
17. Zhang, Y.; Lu, M.; Zhou, Y.; Su, Z.; Liu, B.; Li, G.; Jiang, T. Interfacial Interaction between Humic Acid and Vanadium, Titanium-Bearing Magnetite (VTM) Particles. *Miner. Process. Extr. Metall. Rev.* **2020**, *41*, 75–84. [[CrossRef](#)]
18. Bose, D.K. Pyrometallurgy of Niobium, Tantalum and Vanadium Development Work at Bhabha Atomic Research Centre. *Miner. Process. Extr. Metall. Rev.* **1992**, *10*, 217–237. [[CrossRef](#)]
19. Wang, M.; Huang, S.; Chen, B.; Wang, X. A review of processing technologies for vanadium extraction from stone coal. *Miner. Process. Extr. Metall. Trans. Inst. Min. Metall.* **2020**, *129*, 290–298. [[CrossRef](#)]
20. Yu, J.; Han, Y.; Li, Y.; Gao, P. Beneficiation of an iron ore fines by magnetization roasting and magnetic separation. *Int. J. Miner. Process.* **2017**, *168*, 102–108. [[CrossRef](#)]

21. Bentli, I.; Erdogan, N.; Elmas, N.; Kaya, M. Magnesite concentration technology and caustic–calcined product from Turkish magnesite middlings by calcination and magnetic separation. *Sep. Sci. Technol.* **2017**, *52*, 1129–1142. [[CrossRef](#)]
22. Li, M.; Zheng, S.; Liu, B.; Wang, S.; Dreisinger, D.B.; Zhang, Y.; Du, H.; Zhang, Y. A Clean and Efficient Method for Recovery of Vanadium from Vanadium Slag: Nonsalt Roasting and Ammonium Carbonate Leaching Processes. *Miner. Process. Extr. Metall. Rev.* **2017**, *38*, 228–237. [[CrossRef](#)]
23. Li, W.; Fu, G.; Chu, M.; Zhu, M. An effective and cleaner process to recovery iron, titanium, vanadium, and chromium from Hongge vanadium titanomagnetite with hydrogen-rich gases. *Ironmak. Steelmak.* **2021**, *48*, 33–39. [[CrossRef](#)]
24. Liu, S.; Wang, W.; Yang, J.; You, J. Beneficiation of a low grade titanomagnetite ore in mining engineering. *Adv. Mater. Res.* **2012**, *577*, 187–190. [[CrossRef](#)]
25. Li, X.; Kou, J.; Sun, T.; Guo, X.; Tian, Y. Coal and Coke Based Reduction of Vanadium Titanomagnetite Concentrate by the Addition of Calcium Carbonate. *Miner. Process. Extr. Metall. Rev.* **2021**, *42*, 115–122. [[CrossRef](#)]
26. Xiang, J.; Huang, Q.; Lv, W.; Pei, G.; Lv, X.W.; Liu, S. Co-recovery of iron, chromium, and vanadium from vanadium tailings by semi-molten reduction–magnetic separation process. *Can. Metall. Q.* **2018**, *57*, 262–273. [[CrossRef](#)]
27. Zhang, Z.; Liu, B.; Ma, H.; We, W. Separability of Fe from cyanide tailing by magnetic roasting. *Mater. Sci. Forum* **2011**, *695*, 421–424. [[CrossRef](#)]
28. Luo, X.-f.; Dong, H.; Zhang, S.; Liu, Y.-w. Study on the sodium oxidation properties of low-iron vanadium-titanium magnetite with high vanadium and titanium. *Energy Sources Part A Recover. Util. Environ. Eff.* **2018**, *40*, 1998–2008. [[CrossRef](#)]
29. Dehghan-Manshadi, A.; Manuel, J.; Hapugoda, S.; Ware, N. Sintering characteristics of titanium containing iron ores. *ISIJ Int.* **2014**, *54*, 2189–2195. [[CrossRef](#)]
30. Yang, S.T.; Zhou, M.; Jiang, T.; Wang, Y.J.; Xue, X.X. Effect of basicity on sintering behavior of low-titanium vanadium-titanium magnetite. *Trans. Nonferrous Met. Soc. China* **2015**, *25*, 2087–2094. [[CrossRef](#)]
31. Lv, C.; Yang, K.; Wen, S.-m.; Bai, S.-j.; Feng, Q.-c. A New Technique for Preparation of High-Grade Titanium Slag from Titanomagnetite Concentrate by Reduction–Melting–Magnetic Separation Processing. *JOM* **2017**, *69*, 1801–1805. [[CrossRef](#)]
32. Cheng, G.J.; Xue, X.X.; Liu, J.X.; Jiang, T.; Duan, P.N. Reduction kinetics and mechanism of pellets prepared from high chromium vanadium–titanium magnetite concentrate. *Trans. Inst. Min. Metall. Sect. C Miner. Process. Extr. Metall.* **2017**, *126*, 125–132. [[CrossRef](#)]
33. Zhang, J.; Zhang, W.; Xue, Z. Oxidation Kinetics of Vanadium Slag Roasting in the Presence of Calcium Oxide. *Miner. Process. Extr. Metall. Rev.* **2017**, *38*, 265–273. [[CrossRef](#)]
34. Li, R.; Liu, T.; Zhang, Y.; Huang, J. Mechanism of novel k<sub>2</sub>so<sub>4</sub>/kcl composite roasting additive for strengthening vanadium extraction from vanadium–titanium magnetite concentrate. *Minerals* **2018**, *8*, 426. [[CrossRef](#)]
35. Sui, Y.; Guo, Y.; Jiang, T.; Qiu, G.Z. Separation and recovery of iron and titanium from oxidized vanadium titanomagnetite by gas-based reduction roasting and magnetic separation. *J. Mater. Res. Technol.* **2019**, *8*, 3036–3043. [[CrossRef](#)]
36. Zhao, Y.; Sun, T.; Zhao, H.; Xu, C.; Wu, S. Effect of MgO and CaCO<sub>3</sub> as additives on the reduction roasting and magnetic separation of beach titanomagnetite concentrate. *ISIJ Int.* **2019**, *59*, 981–987. [[CrossRef](#)]
37. Ding, J. Investigation of thermodynamic equilibrium of MSWI fly ash during high-temperature treatment. *Adv. Mater. Res.* **2013**, *610–613*, 1871–1875. [[CrossRef](#)]
38. Arguin, J.P.; Pagé, P.; Barnes, S.J.; Girard, R.; Duran, C. An integrated model for ilmenite, Al-spinel, and corundum exsolutions in titanomagnetite from oxide-rich layers of the Lac Doré complex (Québec, Canada). *Minerals* **2018**, *8*, 476. [[CrossRef](#)]
39. Alkynes, T. Influences of Technological Parameters on Smelting-separation Process for Metallized Pellets of Vanadium-bearing Titanomagnetite Concentrates. *J. Iron Steel Res. Int.* **2016**, *23*, 367–370. [[CrossRef](#)]
40. Tang, W.-d.; Xue, X.-x.; Yang, S.-t.; Zhang, L.-h.; Huang, Z. Influence of basicity and temperature on bonding phase strength, microstructure, and mineralogy of high-chromium vanadium–titanium magnetite. *Int. J. Miner. Metall. Mater.* **2018**, *25*, 871–880. [[CrossRef](#)]